

Inter-annual changes in responses of winter sea-ice motions to winds in the Arctic Ocean between 2003 and 2012

Eri YOSHIZAWA¹ and Koji SHIMADA²

¹ Division of Polar Ocean Sciences, Korea Polar Research Institute, Incheon, Republic of Korea

² Department of Ocean Sciences, Tokyo University of Marine Science and Technology, Tokyo, Japan

(Received September 30, 2016; Revised manuscript accepted December 27, 2016)

Abstract

The response of winter (November–April) sea-ice motions to winds between 2003 and 2012 showed large year to year variations in the southern Canada Basin and the region along the Transpolar Drift Stream. We introduced the anomalies of the areal mean of sea-ice velocity curls averaged for the southern Canada Basin as a proxy of the intensity of the clockwise sea-ice motion in the basin. The composite analysis based on the sea-ice velocity curls showed that the clockwise motion was enhanced when the sea-ice motions in the Alaskan coastal region increased with less sea-ice concentration and the along-shore wind in November–December.

Key words: Arctic Ocean, sea-ice motion, mobility of sea ice

1. INTRODUCTION

In the ice-covered Arctic Ocean, sea-ice motion modulates momentum transfers from atmosphere to ocean. The mean sea-ice velocity in the Arctic Ocean was accelerated anomalously in 2000s, compared to those in 1980s and 1990s, but the wind velocity only partially explained this acceleration (Rampal *et al.*, 2009; Spreen *et al.*, 2011; Kwok *et al.*, 2013). Such changes in the response of sea-ice motions to winds can have a large impact on the underlying upper ocean circulation and associated oceanic heat transports leading to the reduction of winter sea-ice formation (Shimada *et al.*, 2006). Therefore, to investigate what have caused the changes in the kinematic coupling between atmosphere and sea-ice is important for understanding the ongoing sea-ice change.

This study examines the inter-annual changes in the response of sea-ice motions to winds, using passive microwave measurement data from 2003 to 2012. The previous study suggested that the reduced internal stress caused by less sea-ice concentration along the Alaskan coast enhanced the sea-ice motion in the Canada Basin without the significant change in the wind forcing (Shimada *et al.*, 2006). The wind direction against the Alaskan coastline can also affect lateral friction between the sea-ice cover and the coastal boundary, but it was not discussed in the previous study. Thus, we examine the relationship among the response of sea-ice motions to winds, sea-ice concentration and wind field, with a particular focus on the sea-ice motion in the Canada Basin.

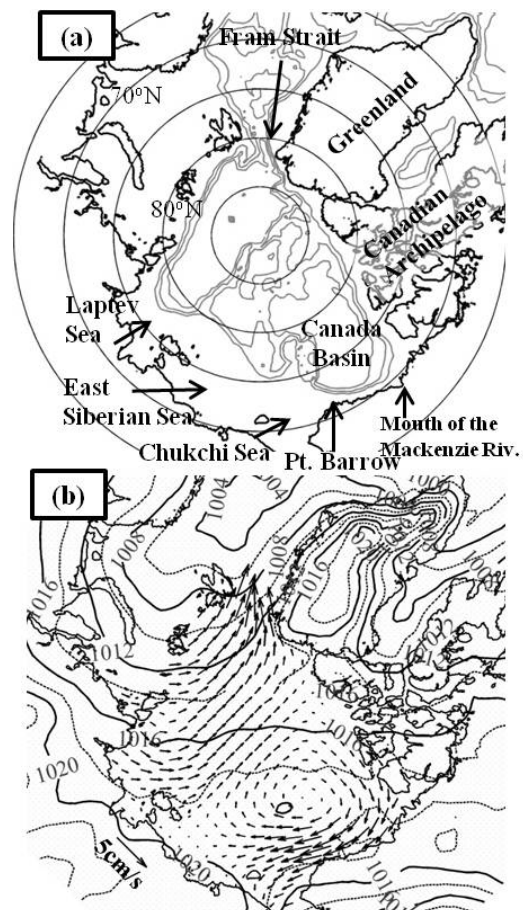


Fig. 1 (a) A map of study region. Schematic seafloor topographies are denoted by gray contours. (b) Winter (November–April) mean fields of sea-ice velocity vectors (vectors; cm/s) and SLP (contours; hPa)

2. DATA

We use sea-ice velocity data from November 2002 to April 2012, which are calculated by the maximum correlation method using brightness temperature images obtained from passive microwave measurements (Kamoshida and Shimada 2010). In the calculation, brightness temperatures observed from the Advanced Microwave Scanning Radiometer for Earth observing system (AMSR-E) are used. In the period other than the AMSR-E operational period, brightness temperatures observed by the Special Sensor Microwave Imager/Sounder (SSMIS) are used. Here, we adopt sea-ice velocity data mapped onto the 43.75×43.75 km grid. We also use sea-ice concentration data provided by the National Snow and Ice Data Center (NSIDC), which is calculated by NASA team algorithm (Cavalieri *et al.*, 1984).

We also use sea-level pressure (SLP) and 10 m wind from the National Centers for Environmental Prediction-National Center for Atmosphere Research (NCEP-NCAR) reanalysis dataset (Kalnay *et al.*, 1996).



Fig. 2 Winter (November-April) mean field of $\nabla \times \vec{u}_i$ (contours; 10^{-7} 1/s). Thin solid (dashed) contours represent positive (negative) values. Thick solid lines represent the zero lines of $\nabla \times \vec{u}_i$.

3. RESULTS

In this study, we focus on the period from November to April, when the mean sea-ice velocity in 2000s reached to its maximum and minimum values (Sprenn *et al.*, 2011). Hereafter, the period is referred to as "winter", e.g., the period from November 2002 to April 2003 is referred to as "the 2003 winter".

First of all, we check briefly characteristics of winter mean sea-ice motions. The map of the study region is shown in Fig. 1a. Figure 1b shows the winter mean fields of sea-ice velocity vectors and SLP in 2003-2012.

The sea-ice velocity vectors exhibit the Transpolar Drift Stream (TDS) of sea-ice motions, which shows the sea-ice advection from the Chukchi Sea to the Fram Strait. Moreover, the clockwise motion is found over the Canada Basin. The sea-ice motions in the region from the southern Canada Basin to the Chukchi Sea are faster than those in the TDS region, but the SLP gradients in the former region are weaker than those in the latter region (contours in Fig. 1b). Figure 2 shows the winter mean field of sea-ice velocity curls ($\nabla \times \vec{u}_i$). The most of the Arctic Ocean is occupied by the negative $\nabla \times \vec{u}_i$, except the Laptev Sea, where the positive $\nabla \times \vec{u}_i$ is evident. The negative $\nabla \times \vec{u}_i$ value shows the local maximum in the southern half of the Canada Basin with flat sea-floor topographies.

Next, we examine the inter-annual variations in the response of sea-ice motions to winds. Kimura and Wakatsuchi (2000) introduced the ratio of sea ice velocities, which are tangential to wind vectors, to wind velocities, in order to reveal the relationship between sea-ice motions and winds. In this study, 10 m wind velocities are used instead of geostrophic winds. Hereafter, this ratio is referred to as "wind factor (WF)". Sea-ice motions are also affected by ocean surface currents. In this study, for simplicity, it is assumed that effects of ocean surface currents are negligibly small compared with those of winds.

Figure 3 shows spatial maps of the winter mean WF from 2003 to 2012. In order to capture changes in the relationship between sea-ice motions and winds in large scales, a 3×3 (131.25×131.25 km) median filter is applied for the WF fields. The previous studies reported that the acceleration of sea-ice motions in 2000s was evident in the southern half of the Canada Basin and the region along the TDS, even the wind speeds were at the almost same level as that in 1980-1990s (Sprenn *et al.*, 2011; Kwok *et al.*, 2013). In these regions, the WF values show the large inter-annual variations from 2003 to 2012, whereas the values in the region north of the Canadian Archipelago remain unchanged (Fig. 3). After the late 1990s, the spatial distributions of sea-ice type varied from year to year in the former regions, while the robust multi-year ice occupied the latter region (Maslanik *et al.*, 2011). Kwok *et al.* (2013) noted that the acceleration of sea-ice motions in the former regions seemed to be associated with the reduction of sea-ice thickness.

Especially, in the southern half of the Canada Basin, the WF values are relatively large ($\sim 1.6\%$) in the winters of 2003, 2004, 2007 and 2008 (Figs. 3a, b, e and f). In these winters, the SLP gradients across the Alaskan coastline from the mouth of the Mackenzie River to Pt. Barrow are stronger than those in the other winters, suggesting that the along-shore winds are predominant (contours in Figs. 3a, b, e and f). As mentioned above, the previous study suggested that the

decreasing in sea-ice concentration in the Alaskan coastal region enhanced the basin-scale clockwise sea-ice motion (Shimada *et al.*, 2006).

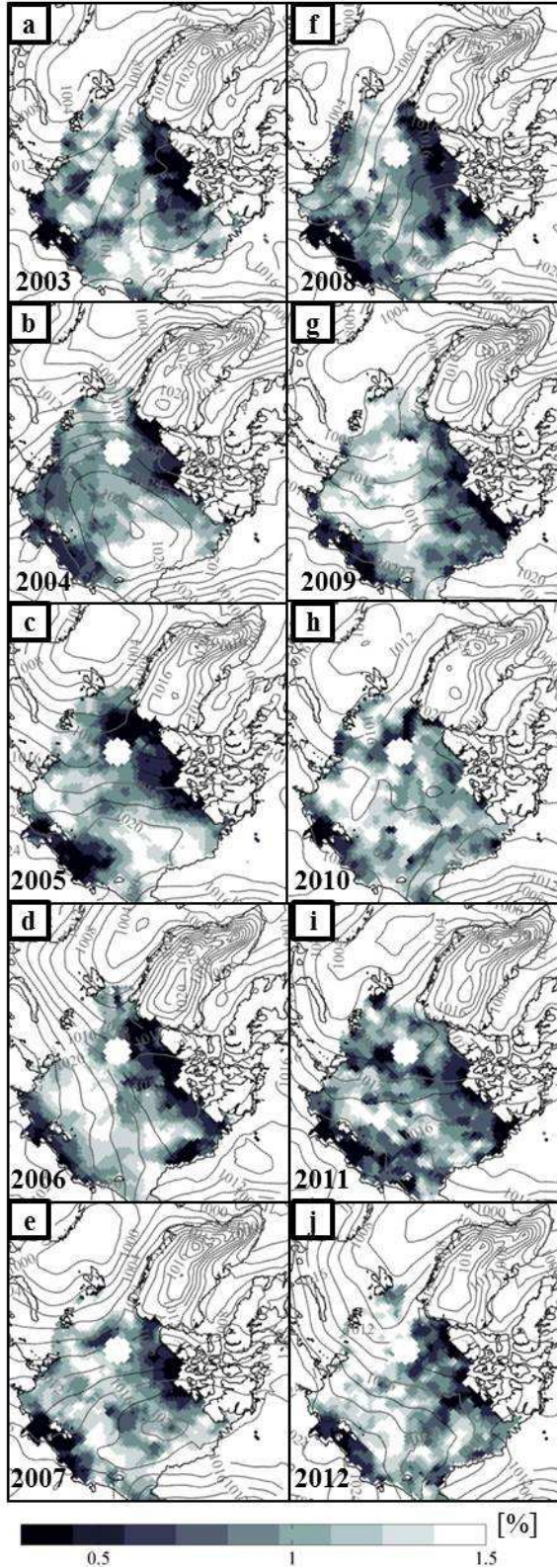


Fig. 3 Winter (November-April) mean fields of WF (%) with SLP (contours; hPa)

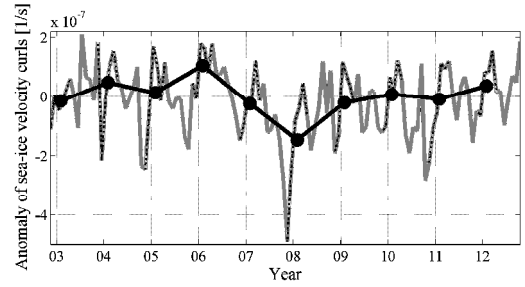


Fig. 4 Time series of the $\nabla \times \bar{u}_i$ index from 2003 to 2012. A black (gray) solid line is winter means (monthly means) of the index

Therefore, to extract the relationship among the intensity of the clockwise sea-ice motion and other parameters (sea-ice concentration and wind direction against the coastline), we employ the composite analysis based on $\nabla \times \bar{u}_i$.

We note again that there is the local minimum value of $\nabla \times \bar{u}_i$ in the southern Canada Basin (dashed contours in Fig. 2). It has been reported that the clockwise sea-ice motion was predominant in the Canada Basin throughout the year except the late summer (McLaren *et al.*, 1987; Asplin *et al.*, 2009). Similarly, during 2003 to 2012, the monthly mean values of $\nabla \times \bar{u}_i$ averaged for the southern Canada Basin (73-77°N, 130-160°W) show the negative value except the summers of 2003 and 2008 (not shown). Thus, we use anomalies of areal mean values of $\nabla \times \bar{u}_i$ in this region as a proxy of the intensity of the clockwise sea-ice motion in the Canada Basin (hereinafter referred to as "the $\nabla \times \bar{u}_i$ index"). In this study, it is assumed that the intensity of the clockwise motion is strong (weak) when the $\nabla \times \bar{u}_i$ index is negative (positive).

Figure 4 shows the time series of the winter mean values of the $\nabla \times \bar{u}_i$ index (thick black line) with the monthly mean values (gray line). In the inter-annual time scale, the intensity of the clockwise sea-ice motion in winter reaches its maximum value in 2008 and then recovered to the same level of the early 2000s (black solid line in Fig. 4). Using this index, we make two composites of WF and SLP when the index is below (above) zero. The composite with the negative index is constructed from the data in the five winters (2003, 2007, 2008, 2009 and 2011), and the composite with the positive index is constructed from the data in the other five winters (2004, 2005, 2006, 2010 and 2012). Since the inter-annual variability of WF is large in November-December compared with that in January-April (not shown), we here use the WF values averaged in November-December.

Figure 5 shows the two composite maps of WF with SLP. In the negative index composite, the WF values are relatively large in the Chukchi Sea and the southern half of the Canada Basin (Fig. 5a). In the positive index

composite, the values are also large in the Chukchi Sea, but the values are small in the Canada Basin except the coastal area just east of Pt. Barrow (Fig. 5b). The difference in the WF values between the two composites also indicates that the clockwise motion is enhanced when the WF values are large in the southern Canada Basin (Fig. 6a). In the region along the Alaskan coast, sea-ice concentration in the negative index composite is lower, compared with that in the positive index composite (Fig. 6b). The results confirm the relationship between the intensity of the basin-scale sea-ice motion and the lateral boundary condition along the Alaskan coast, which was pointed by Shimada *et al.* (2006).

If the wind that is along (perpendicular to) the Alaskan coastline from the mouth of the Mackenzie River to Pt. Barrow is dominant, the basin-scale clockwise sea-ice motion would accelerate (deaccelerate) due to decreases (increases) in lateral friction between the ice-cover and the Alaskan coastal boundary. Focusing on the Canada Basin along the 75°N line, the mean SLP field denoted by contours in Fig. 5a (Fig. 5b) shows that the wind in this region is nearly parallel to (intersects with) the coastline when the WF values are relatively large (small) in the southern portion of the basin. This implies that the direction of the wind in the southern Canada Basin is one of the key conditions to promote effective kinematic coupling between sea-ice motions and winds in the Canada Basin.

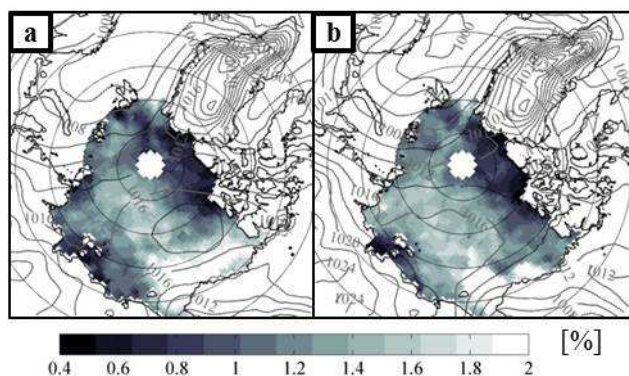


Fig. 5 Spatial maps of WF (%) and SLP (contours; hPa) in November-December averaging when (a) the $\nabla \times \vec{u}_i$ index is below zero and (b) above zero

4. CONCLUSIONS

This paper indicated that the response of sea-ice motions to 10 m winds in winter varied largely from year to year in the southern half of the Canada Basin and the TDS region from 2003 to 2012. In this study, we particularly focused on the clockwise sea-ice motion in the Canada Basin, and attempted to investigate what controlled the intensity of the clockwise motion. We introduced the anomalies of the

areal mean values of $\nabla \times \vec{u}_i$, averaged for the southern Canada Basin, where the $\nabla \times \vec{u}_i$ value showed its local minimum, as a proxy of the intensity of the clockwise sea-ice motion. The composite analysis based on $\nabla \times \vec{u}_i$ indicated that the intensity of the clockwise motion was large when the WF values were large in the southern half of the basin near the Alaskan coast compared with those in the other regions. In the case that the intensity of the clockwise motion was strong (weak), sea-ice concentration near the Alaskan coast was low (high) and the wind in the southern Canada Basin was nearly parallel to (intersected with) the Alaskan coastline in the early winter (November-December).

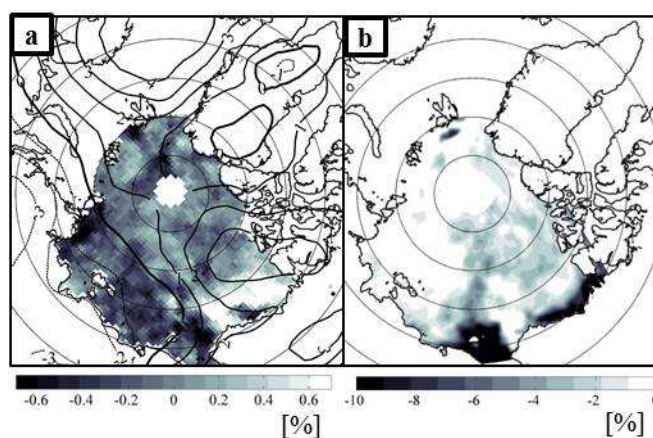


Fig. 6 (a) Differences between the two composites (the negative index composite minus the positive index composite) in (a) WF (%) with SLP (contours; hPa) and (b) sea-ice concentration (%) in November-December

REFERENCES

- Asplin, M. G., J. V. Lukovich and D. G. Barber (2009): Atmospheric forcing of the Beaufort Sea ice gyre: Surface pressure climatology and sea ice motion, *J. Geophys. Res.*, **114**, C00A06, doi:10.1029/2008JC005127.
- Cavalieri, D. J., P. Gloersen and W. J. Campbell (1984): Determination of sea ice parameters with the NIMBUS 7 SMMR, *J. Geophys. Res.*, **89**(D4), 5355–5369.
- Kalnay, E. and 21 other authors (1996): The NCEP/NCAR 40-year reanalysis project, *Bull. Am. Meteorol. Soc.*, **77**, 437–471.
- Kamoshida T. and K. Shimada (2010): Long term sea ice motion dataset in the Arctic from SMMR, SSM/I and AMSR-E. In: Proceedings of the second international symposium on the Arctic research, Tokyo, Japan, 2010, p 125.
- Kimura, N. and M. Wakatsuchi (2000): Relationship between sea-ice motion and geostrophic wind in the Northern Hemisphere, *Geophys. Res. Lett.*, **27**, 3735–3738.
- Kwok, R., G. Spreen and S. Pang (2013): Arctic sea ice circulation and drift speed: Decadal trends and ocean currents, *J. Geophys. Res. Oceans*, **118**, 2408–2425, doi:10.1002/jgrc.20191.
- McLaren, A. S., M. C. Serreze and R. G. Barry (1987): Seasonal variations of sea ice motion in the Canada basin and their

- implications, *Geophys. Res. Lett.*, **114**:1123–1126.
- Maslanik, J. and 3 other authors (2011): Distribution and trends in Arctic sea ice age through spring 2011, *Geophys. Res. Lett.*, **38**, L13502, doi:10.1029/2011GL047735.
- Rampal, P., J. Weiss and D. Marsan (2009): Positive trend in the mean speed and deformation rate of Arctic sea ice, 1979–2007, *J. Geophys. Res.*, **114**, C05013, doi:10.1029/2008JC005066.
- Shimada, K. and 7 other authors (2006): Pacific Ocean inflow: Influence on catastrophic reduction of sea ice cover in the Arctic Ocean, *Geophys. Res. Lett.*, **33**, L08605, doi:10.1029/2005GL025624.
- Spreen, G., R. Kwok and D. Menemenlis (2011): Trends in Arctic sea ice drift and role of wind forcing: 1992–2009, *Geophys. Res. Lett.*, **38**, L19501, doi:10.1029/2011GL048970.